Does long-term radiation exposure in Chornobyl impact the reproductive structures of Nuphar lutea (Linné) Smith?

Lesya Zub, Mariana Prokopuk, Maksym Netsvetov, Dmitri Gudkov

[1]Does long-term radiation exposure in Chornobyl impact the reproductive structures of *Nuphar lutea* (Linné) Smith?

Lesya Zub[a], Mariana Prokopuk[a]*, Maksym Netsvetov [b,c], Dmitri Gudkov [d]

[a] *Laboratory of Preservations and Biodiversity Renewal, Institute for Evolutionary Ecology, National Academy of Sciences of Ukraine, Kyiv, Ukraine*

[b] *Department of Phytoecology, Institute for Evolutionary Ecology, National Academy of Sciences of Ukraine, Kyiv, Ukraine*

[c] *BIOGECO, University of Bordeaux, INRAE, Cestas, France*

[d] *Department of Aquatic Radioecology, Institute of Hydrobiology, National Academy of Sciences of Ukraine, Kyiv, Ukraine*

Abstract

The 1986 Chornobyl Nuclear Power Plant accident caused radioactive contamination of water bodies within the Pripyat River floodplain, resulting in the accumulation of radionuclides by macrophytes, which are fundamental species in water ecosystems. Yellow water lily *Nuphar lutea* (L.) Smith., a macrophyte playing a significant role in the formation of vegetation cover in aquatic ecosystems, is commonly considered as a bioindicator of water pollution. In this study, we investigate the potential of *N. lutea* as an indicator of radionuclide contamination in water bodies, particularly through changes in its reproductive structures, such as pollen viability, morphology of pollen grains, seeds, and fruits. Our findings reveal that pollen viability remains stable at total absorbed dose rates below 14.4 μGy/h, with only 1-4% of sterile grains. However, beyond this threshold the percentage of sterile grains increases nearly fivefold, pointing to high internal plant

* Corresponding author. E-mail address: maryanaprokopuk406@gmail.com (M. Prokopuk).

exposure to ^{90}Sr. A similar trend was observed in the allometry and size of pollen grains, where small and flattened grains are formed in the reservoir with the highest external radiation dose rate (≥ 14.4 μGy/h). On the other hand, while morphometric parameters of fruits are influenced by radiation, their variation appears to be the result of a combination of physicochemical factors and the trophic status of a water body. Our research highlights the adverse impact of long-term radiation exposure on the male reproductive system of *N. lutea* and shows the potential of using the pollen grains sterility as an indicators of heavily radionuclide-contaminated water bodies. Additionally, we observed gradual changes in a pollen allometric length-to-width coefficient as the radiation dose level increases.

Keywords: Chornobyl exclusion zone, water bodies, *Nuphar lutea,* radionuclide contamination, absorbed dose rate, pollen grains, dose-dependent changes

1. Introduction

Following the Chornobyl Nuclear Power Plant (CNPP) accident, the floodplain of the Pripyat River experienced substantial radionuclide contamination. The Chornobyl Exclusion Zone (CEZ), an area of about 2,600 km² surrounding CNPP, encompasses diverse water bodies, including rivers, lakes, backwaters, streams, and canals. These shallow aquatic environments are characterized by the prevalence of aquatic macrophytes – large, visible plants that primarily grow in permanently or periodically submerged areas (Thomaz et al., 2009). Due to their

significant capacity for absorbing radioactive substances, macrophytes play a pivotal role in the biogeochemical cycling and redistribution of radionuclides within aquatic ecosystems (Fukuda et al., 2014; Ganzha et al., 2014, 2020; Gudkov et al., 2002; Gudkov et al., 2003; Klochenko et al., 2008). Additionally, they are commonly employed in monitoring studies to assess the contamination of water bodies by radionuclides (Gudkov et al., 2006; Gudkov et al., 2003).

Aquatic plants exhibit a remarkable ability to adapt their traits to changing habitats, resulting in a high degree of phenotypic plasticity and local adaptations (Dorken and Barrett, 2004; Keddy et al., 2000; Puijalon and Bornette, 2004; Santamaría, 2002; Titus and Gary Sullivan, 2001; Yuan et al., 2024; Wells and Pigliucci, 2000). Long-term radiation exposure within the CEZ elicits responses in aquatic plants, indicating damages or alterations at multiple organizational levels (Iavniuk et al., 2020; Nurgudin et al., 2009; Shevtsova and Gudkov, 2009; Tsyusko et al., 2006; Yavnyuk et al., 2009). The extensive effects of chronic ionizing radiation exposure (Gudkov et al., 2006; Gudkov et al., 2016; Mousseau and Møller, 2020) underscore the importance of investigating responses dose-dependent reactions in aquatic macrophytes.

Nuphar lutea (L.) Smith, commonly known as the yellow water-lily, is a fundamental species shaping the vegetation cover of water bodies within the CEZ (Zub et al., 2023). Monodominant communities of *N. lutea* are widespread in the shallow waters of large and shallow lakes, while ephemeral communities associated with *Stratiotes aloides* L. can be found in abandoned channels with muddy

sediments along the shores (Zub et al., 2023). In addition, *N. lutea* metal absorption capacity (Polechońska et al., 2022) highlights its potential use in biomonitoring studies of radionuclide-contaminated water bodies.

One of the key factors determining a species' resilience to adverse environmental conditions is the viability of its reproductive structures, specifically pollen grains. The male gametophyte is highly sensitive to various environmental pollutants (De Storme and Geelen, 2014; Hjelmroos, 2000; Jefferies, 1977; Kurtar, 2009; Mičieta and Murín, 1996; Mulcahy, 1981; Murin and Micieta, 1998), particularly radionuclides resulting in chronic radiation exposure for plants (Blasco et al., 2016; Møller et al., 2016; Møller and Mousseau, 2017). This vulnerability is evidenced by an increase in the proportion of nonviable pollen grains and a decrease in their fertility. Exposure to adverse conditions can also lead to observable variations in the morphology of pollen grains and other reproductive structures in aquatic plants, serving as indicators of environmental toxicity.

The objective of this study is to investigate the effects of long-term ionizing radiation on the fertility and pollen morphology of *N. lutea*, as well as the traits of its seeds and fruits. Although seed dispersal is not a critical factor for *N. lutea* reproduction, we hypothesized two key points: (i) the sensitivity of its male gametophyte is dose-dependent concerning radioactivity, and (ii) fruit morphology and seed quality may serve as indicators of the absorbed dose rate experienced by the plant.

2. Material and methods

2.1. Biological and aquatic research objects

The investigation involved *N. lutea* specimens from five reservoirs within the CEZ, each characterized by varying absorbed dose rates. Additionally, we examined a reference reservoir with a low background level of radioactive contamination. This study was centered on the analysis of pollen grains, fruits, and seeds from *N. lutea*. Specimens were collected from five reservoirs in the CEZ between 2020 and 2021. Specifically, our study encompassed the following locations: Hlyboke (formerly referred to as Glyboke or Glubokoye) (51°26'37.24"N, 30°3'48.72"E), Vershyna (51°25'58"N, 30°4'23"E), Daleke (51°25'46"N, 30°6'10"E), Plyutovyshche (51°15'12"N, 30°16'24"E), and Yanivskiy Backwater (51°24'28"N, 30°5'5"E). To serve as a reference, we selected a floodplain reservoir of the same type (50°20'3"N, 30°35'1"E) with minimal background radionuclide contamination. This reservoir is situated within the estuary of the Konyk River, a right tributary of the Dnipro River, and falls within the local landscape reserve (LR) known as “Zhukiv Ostriv“ (referred to as LR “Zhukiv Ostriv“ Lake in the text) (Fig. 1). Located within a protected area, this reservoir is still almost untouched by human activity and shares similar hydrological and hydrochemical characteristics with other water bodies under study.

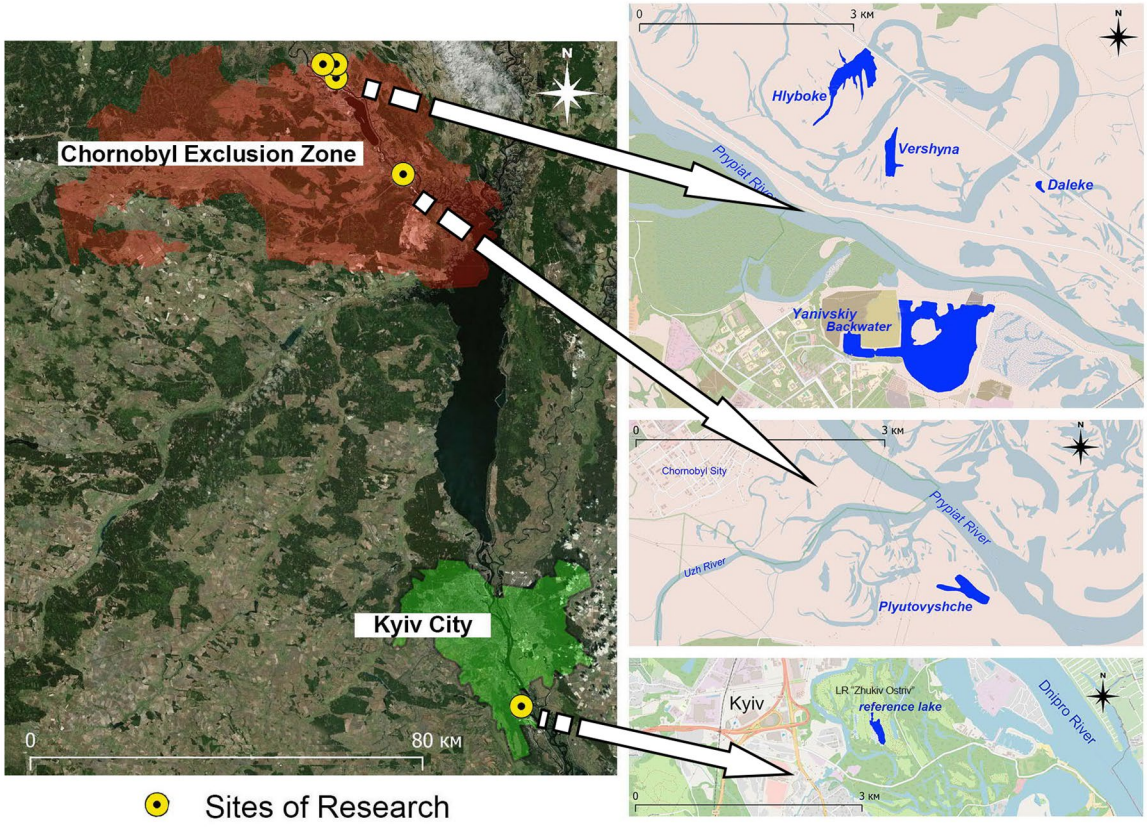

111

112 **Fig. 1.** Scheme of the location of research reservoirs.

113 The studied water bodies are exposed to a wide range of radionuclide
114 contamination, resulting in varying radiation absorbed dose rates for aquatic
115 macrophytes. These differences primarily arise from their geographical positioning
116 withing the CEZ, their proximity to the destroyed CNPP unit, and the intensity of
117 radioactive fallout in the surrounding area during the active phase of the accident in
118 1986.

119 Yanivskiy Backwater, Daleke, Vershyna and Hlyboke lakes are all situated
120 within the 10-km exclusion zone at a distance 3.2, 4.6, 5.3 and 6.7 km from the
121 CNPP, respectively. These water bodies were directly exposed to the north-western
122 radioactive emission during the accident at the 4th unit. Yanivskiy Backwater

123 located on the right bank of the Prypiat River, had been connected to the Pripyat
124 River before the accident. However, due to extensive radiactive contamination it was
125 separated from the Pripyat riverbed using sandbags and later by a dike. Nonethless,
126 compared to the lakes of the left bank of the Pripyat River floodplain, the
127 hydrological connection between the backwater and the river has been substantially
128 higher, resulting in a faster cleanesing of radionuclides from the water and leading
129 to a relatively low dose rate for plants during the study period.

130 Vershyna and Hlyboke lakes are situated in the dammed section of the left-
131 bank floodplain of the Prypiat River and experienced the highest level of
132 radionuclide deposition, while Plyutovyshche Lake, located 24 km from the CNPP,
133 has the lowest levels of radionuclide contamination.

134

135 *2.2. Radiation dose rate assessment*

136

137 The assessment of the total radiation dose rate for *N. lutea* was conducted
138 based on calculated external and internal exposure of studied plants (see Table 1).
139 For external radiation dose rate measuments, we used Na-I field radiometer SRP-
140 68-03 (Prompribor, Russia) for performing studies in aquatic environments.
141 Measurements were carried out at the surface, in different layers of the water
142 column, and also up to 10 cm deep into bottom sediments. Internal radiation dose
143 rate calculations were based on the activity concentration of the main dose-
144 contributing radionuclides within the plant tissues – ^{137}Cs and ^{90}Sr. For these

purposes plants were sampled as a whole (a rhizome fragment 30-40 cm long with leaves and peduncles) in the littoral zone of water bodies up to 25 m long from a depth of 50-80 cm. To measure the radionuclide content, 10-15 plant samples were used for each reservoir. The concentration of ^{137}Cs was measured using a γ-spectrometry complex: PGT IGC-25 detector (France), Nokia LP 4900 B analyser (Nokia, Finland), low-voltage power source, NIM BIN crate, amplifier NU-8210 (Elektronicus Merokeszulekek Gyara, Hungary) and 100mm-thick lead shield.

Table 1

Components of the average total absorbed dose rate to *Nuphar lutea* in studied water bodies, μGy/h.

Water body	External	Internal ^{90}Sr	Internal ^{137}Cs	Total
Vershyna Lake	7.49±3.01	6.84±0.89	0.06±0.01	14.39±3.04
Hlyboke Lake	8.14±3.06	2.31±1.28	0.30±0.09	10.75±3.15
Daleke Lake	1.43±0.27	1.32±1.15	0.22±0.08	2.97±1.10
Yanivskiy Backwater	1.65±0.65	0.27±0.13	0.03±0.01	1.95±0.48
Plyutovyshche Lake	0.19±0.08	0.039±0.009	0.004±0.001	0.233±0.075
LR “Zhukiv ostriv” Lake	0.08±0.01	0.001±0.0003	0.0003±0.0001	0.081±0.010

The concentration of ^{90}Sr was measured on a low-background NRR-610 β-radiometer (Tesla, Czech). Minimal detectable activity was 0.04 Bq after 1000 s of counting. The measurement results are given in Bq/kg at natural humidity; the error of estimated radionuclide concentration fell within 15–25%. The average activity

concentrations for both radionuclides on whole body of *Nuphar lutea* within the studied reservoirs are given in Table 2.

Table 2

Average activity concentration of radionuclides in *Nuphar lutea* in studied water bodies, Bq/kg at natural humidity.

Water body	Activity concentration	
	^{90}Sr	^{137}Cs
Vershyna Lake	14100±1609	484±117
Hlyboke Lake	4712±2599	2409±654
Daleke Lake	2679±2285	1851±1292
Yanivskiy Backwater	556±320	254±167
Plyutovyshche Lake	81±18	33±11
LR “Zhukiv ostriv” Lake	2.1±0.6	2.4±0.7

Dose rate from incorporated radionuclides using ERICA Assessment Tool 2.0. The integrated approach seeks to combine exposure/dose/effect assessment with risk characterization and managerial considerations (ERICA Assessment Tool 2.0, 2023)

2.3. Reproductive structures study

Pollen analysis included the assessment of fertility and sterility in *N. lutea* pollen, coupled with a comparison of morphometric parameters of pollen grains across water bodies exposed varying degrees of radioactive contamination. Pollen samples were collected during the peak flowering period. Fertility assessments were conducted using the iodine method, a technique for detecting starch in mature pollen grains (Jefferies, 1977). Fertile pollen grains exhibited dark purple coloration, while sterile pollen grains remained uncoloured, as they either contained no starch or only traces of it (Fig. 2 B).

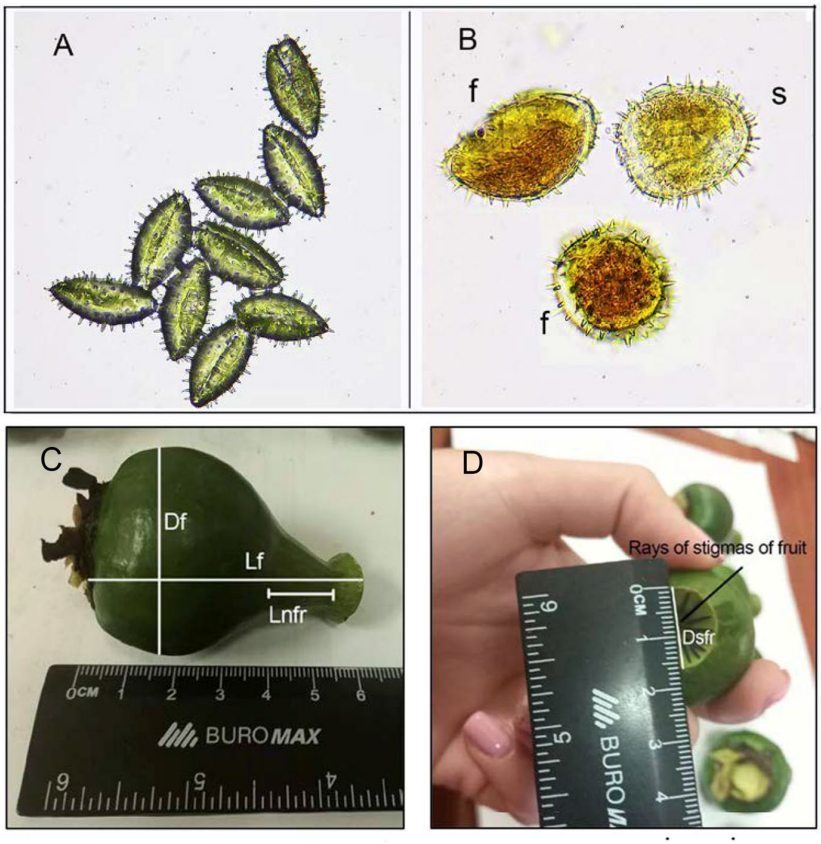

Fig. 2. View of *Nuphar lutea* pollen under a microscope (40x magnification): A – general view of pollen grains, B – stained pollen (where: f – fertile grains, s – sterile grains) C, D – the main morphometric parameters of the fruits that were measured.

186 Flowers and fruits of *N. lutea* (10-15 samples from each water body) were
187 collected from different parts of studied reservoir, including coastal shallow waters
188 and central areas. We analysed 800-1000 pollen grains from each sample, using 70-
189 80 repetitions of the field of view with an Ulab XY-B2N LED microscope. To
190 facilitate morphometric studies of pollen grains, seeds, and fruits, images
191 acquisition, processing, and analysis were provided using AxioVision Rel.4.8
192 software. Specifically, we measured the dimentions of pollen grains (length Lp and
193 width Wp), seeds (Ls, Ws), as well as fruits length (Lfr), diameter (Dfr), neck length
194 (Lnfr), stigma diameter (Dsfr) (Fig. 2 C), and the number of stigma rays (Nsr) (Fig.
195 2 D). Additionally, we calculated the number of seeds (Nsfr) in each pod. Fruit
196 morphometry was carried out for lakes Hlyboke, Daleke, Plyutovyshche, Yanivsky
197 Backwater and the reference "Zhukiv Ostriv" Lake. However, it's worth noting that
198 due to the limited population size of *N. lutea* in Vershyna Lake the detection of pods
199 was not feasible, and consequently, the fruit morphometric study was not provided
200 for this particular reservoir.
201 To analyse the environmental conditions and determine the trophic status of
202 the reservoirs, we conducted hydrochemical studies, focusing on the content of key
203 nutrients (NO_2^-, NO_3^-, NH_4^+, PO_4^{3-}) and the assessment of total mineralisation of the
204 reservoir (Table 3). Biogens analysis was performed by the colorimetric method
205 using the DR/890 Colorimetre. Water samples were collected during the summer
206 month within the *N. lutea* communities.
207

208

209

210

211 **Table 3**

212 Results of the hydrochemical analysis of the water in the studied reservoirs (Standard

213 photometric deviation ±0.005).

Water object	Date	NH_4^+, mgN/dm^3	NO_2^- mgN/dm^3	NO_3^-, mgN/dm^3	PO_4^{3-} mgP/dm^3	Total mineralisation
Vershyna Lake	22.08.2020	0.076	0.090	0.18	0.57	157.93
Hlyboke Lake	21.08.2020	0.010	0.071	0.28	2.36	148.70
Daleke Lake	22.08.2020	0.020	0.023	0.49	0*	135.53
Yanivskiy Backwater	24.08.2020	0.050	0.010	0.74	0.32	143.18
Plyutovyshche Lake	25.08.2020	0.020	0.010	0.25	0	97.70
LR "Zhukiv ostriv" Lake	25.08.2020	0.260	0.001	0.09	1.47	195.36

214 * - below the analised level

215

216 *2.4. Statistical data processing*

217

218 To analyse pollen morphology, we employed centered principal component

219 analysis (PCA) and one-way multiple analysis of variance (MANOVA). When

220 dealing with mising values in morphometric data, we substituted them with the site-

221 mean values to facilitate PCA.

222 To assess the relationships between environmental variable and
223 morphological parameters in studied water bodies, Coinertia Analysis was carried
224 out based on the two tables obtained in PCAs applied to respective datasets (Doledec
225 and Chessel, 1994). PCA was performed on pollen data collected from all six water
226 bodies, while CoA was conducted on pollen, seed, and fruit measurements from five
227 of the studied water bodies as the fruit morphometric data was absent in the
228 Yanivsky reservoir.

229 Following MANOVA, we conducted post-hoc univariate one-way Analysis
230 of Variance (ANOVA) test to identify the variables that contributed to the overall
231 difference among sites. Subsequently, Tukey pairwise comparisons test was
232 performed to determine specific differences between pairs of sites. We applied
233 Bonferroni multiple testing correction in multiple post-hoc examinations. To
234 compare the proportion of fertile and sterile pollen at studied sites we used the two-
235 sided exact Fisher's test. We utilised R-software's 'ade4' and 'car' packages for
236 PCA/CoA and MANOVA.

237

238 **3. Results and discussion**

239

240 A preliminary analysis of the results showed relative resistance of pollen
241 grains to radiation exposure. Only in the reservoir with the highest absorbed dose
242 rate (14.39 μGy/h) – Vershyna Lake – the rate of sterile grains was 18%, while in

243 the rest of the reservoirs it did not exceed 1-4% (Fig. 3, Table S1). The result of the
244 Fisher's exact test ($p>0.001$) says the six sites have the different pollen viability.

245 Only one species of *Nuphar*, *N. lutea*, is represented in all reservoirs in the
246 study area. This is why we rejected the hypothesis of hybridisation affecting pollen
247 grain diversity, as noted by other researchers (Arrigo et al., 2016; Padgett et al.,
248 1998). *N. lutea* is one of the macrophytes that can concentrate radionuclides in
249 significant quantities, primarily ^{137}Cs (second-order concentrator) (Gudkov et al.,
250 2003; Gudkov et al., 2002). This is due to the ability of the species to accumulate
251 relatively large amounts of potassium, which is a chemical analogue of Cs, in its
252 tissues – up to 30.02 g/kg (rhizomes and roots) 29 g/kg (leaves) of dry plant mass
253 (Tomaszewicz and Ciecierska, 2011). The ability of pollen grains to accumulate Ca
254 in their shells is important in terms of forming a dose to plant reproductive structures
255 (Butowt et al., 1997; Tian et al., 1998). Ca is a chemical analogue of Sr, and its
256 radioactive isotope (^{90}Sr) forms the overwhelming part of the radionuclide
257 contamination and internal dose to macrophytes in the CEZ (Gudkov et al., 2009,
258 Gudkov et al., 2002; Kashparov, 1998).

259
260
261
262
263

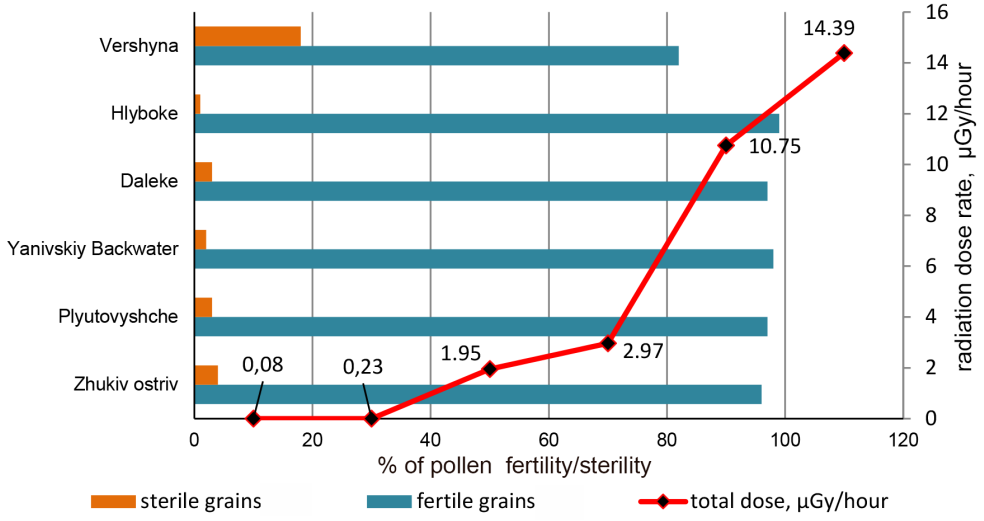

Fig. 3. Viability of *Nuphar lutea* pollen grains in the gradient of the absorbed dose rate.

The total absorbed dose rate of radiation exposure does not significantly affect the range of pollen grains dimentions. Nevertheless, we observed the smallest pollen grains, both in terms of length and width, within the reservoir characterised by the highest external radiation dose rate – Vershyna Lake (Fig. 4, Table S1). In contrast, in the other reservoirs the grains were 10–14% larger; their dimensions were similar. Across all water bodies, we documented a wide range of values in the morphometric indices of pollen grains, with some variations reaching nearly double the size, e.g., Yanivskiy Backwater Lp_{max}=74,43 µm, Lp_{min}=37,05 µm; Wp_{max}=48,23 µm, Wp_{min}=25,16 µm.

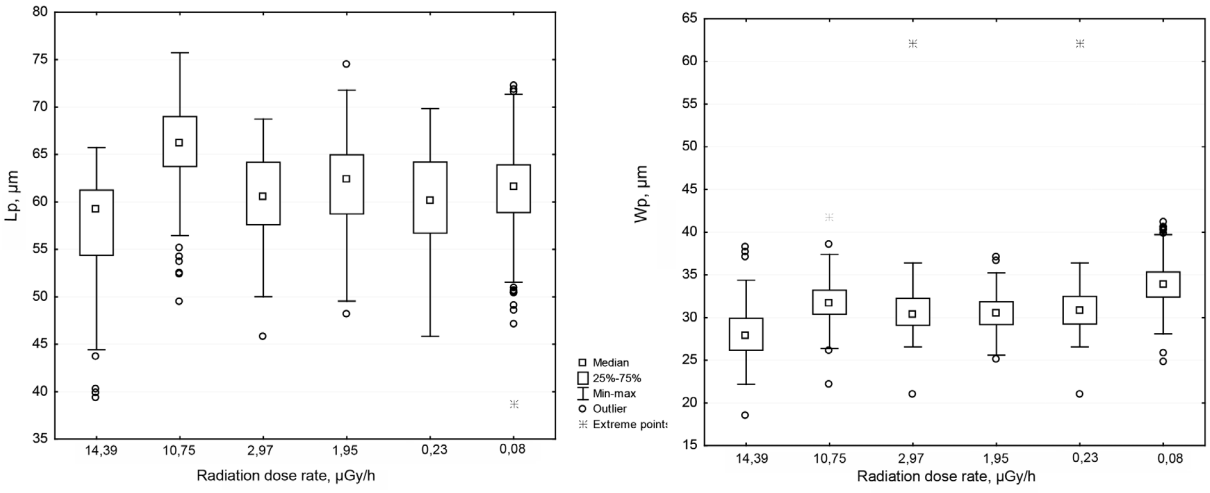

Fig. 4. Diagrams of the range of morphometric parameters of *Nuphar lutea* pollen grains in gradient of radation dose rate: left side – length of pollen grains, right side – width of pollen grains.

Fig. 5 shows the results of PCA applied to pollen morphology and fertility data. In the correlation circle (left side of a figure), the first axis reflects the gradient in the Lp/Wp ratio, with its highest values set toward the left side. The second axis mainly associated with a gradient of fertility (Fert), but it also related to Lp and Wp separated by the first axes.

The factor map (Fig. 5, right side) shows the groupping of the six water bodies marked by inertia ellipses. Vershyna Lake, with the the highest radioactive contamination, stands at the most distinct position. Its projection toward the bottom left part of the factor map corresponds to high values of Lp/Wp ratio and low fertility. Having the second highest exposition level, Hlyboke Lake sets at the top left part of the map implying high pollen fertility. “Zhukiv Ostriv” sets a position at the right side, indicating higher Lp/Wp ratio. The projections of the other sites cluster around the center of coordinates, showing their relatively average parameters values among all sites.

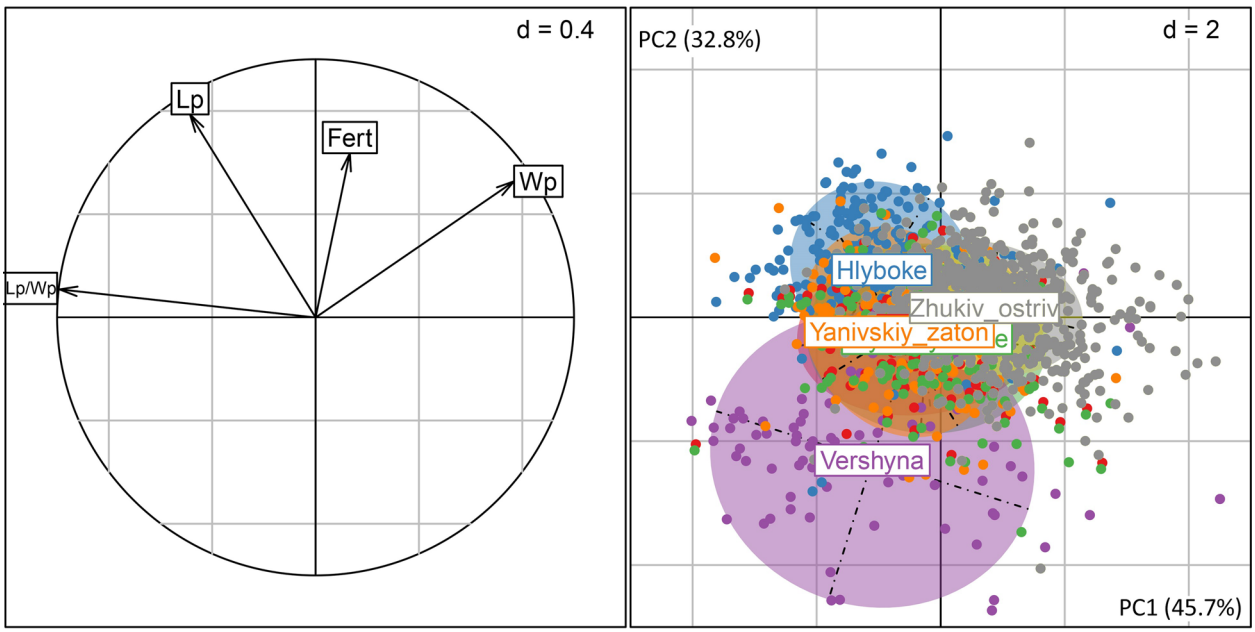

293 **Fig. 5.** PCA of the pollen morphology and fertility data. Left: parameters
294 correlation circle. Right: PCA sites factor map, with samples grouped for each
295 water body. Ellipses are inertia ellipses highlighting ~68% samples of each group
296 projection on axes (Lp is the length of a grain; Wp is the width of grain; Lp/Wp is
297 the length-to-width ratio; Fert is the pollen grains fertility).
298
299 The results of MANOVA confirmed the significant differences (p-value <
300 0.001) among the sites. Subsequent post-hoc tests showed there was a significant
301 difference (p-value < 0.05) in each studied pollen parameter between the sites.
302 Further pairwise comparison revealed that the most prominent differences were
303 observed between Vershyna Lake, Hlyboke Lake, and "Zhukiv Ostriv" when
304 compared to other sites (Table S1).
305 Pollen shape index (Lp/Wp) showed gradually grows with the increase of
306 the radiation dose rate (Fig 6). A strong relationship (R^2=0.86) was found between
307 the size of pollen grains and the total absorbed dose rate, suggesting the dose-
308 dependent influence of radioactive contamination on the reproductive structures of
309 plant. With the increase of absorbed dose rate, the size of pollen grains decreases
310 (the value of Lp/Wp for the control is 1.81, while for the most contaminated water
311 body – Vershyna Lake – it was 2.04). Thus, pollen grains have the smallest size in
312 the water body with the highest dose rate to the plants.

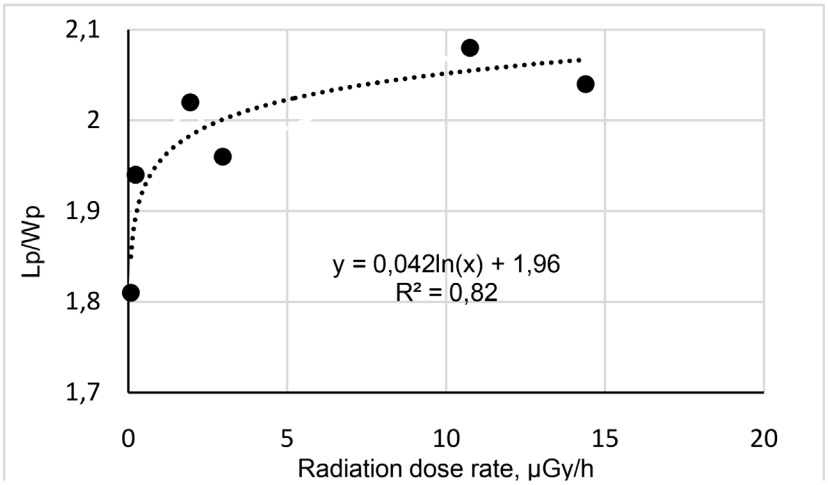

Fig. 6. The dependence between total radiation dose rate and pollen grain length-to-width ratio (average values for water bodies).

As shown in Fig. 6, when the Lp/Wp ratio exceeds >1.9, it indicates the radioactive contamination of the environment. This increased ratio signifies a reduction in the reproductive capacity of local populations resulting from radiation pollution. Notably, the Lp/Wp ratio is sensitive to low radiation doses, with discernible changes in pollen grains observed in Plyutovyshche Lake at a dose as low as 0.233 µGy/h.

The results of the Coinertia Analysis are shown in Fig. 7. The projection of the first axes of the two separate PCAs for environmental variables and morphological datasets onto the coinertia axes reflects relationships between the ain structures of each dataset and co-structure obtained in Coinertia Analysis. The coinertia axes are not equivalent to the axes of both the environmental and morphological PCAs, necessitating an axis rotation (as indicated by the circles in the top left of Fig.8).

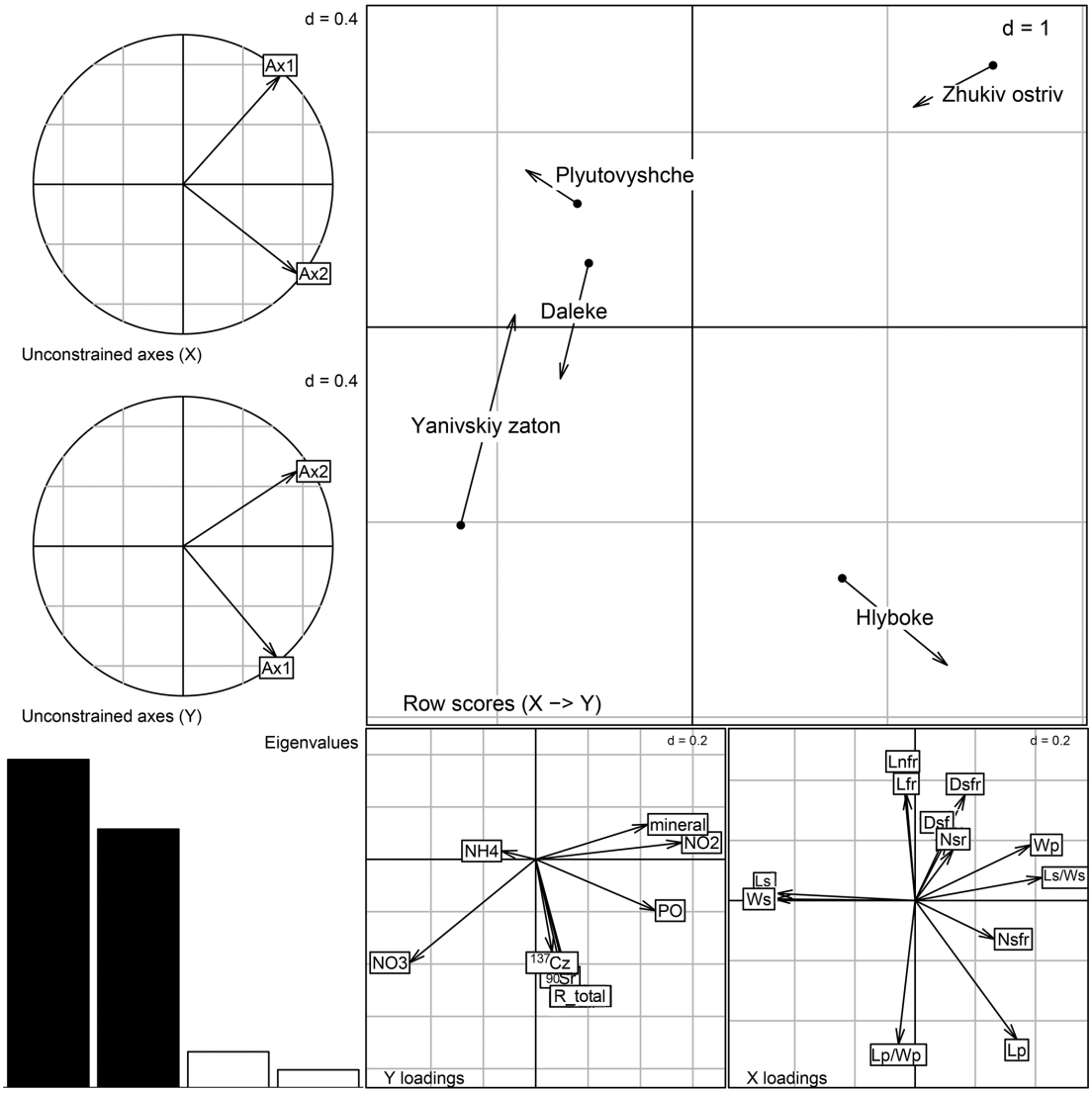

334 **Fig. 7**. Composite plot of Coinertia Analysis performed for environmental
335 variables and pollen, fruits, seeds morphology datasets. The projection of the first
336 axes of the two simple PCA for environmental variables and morphological data
337 onto the coinertia axes at the top left. The combined plot of site's scores of
338 environmental conditions (arrows) and morphological dataset (points). The barplot
339 of eigenvalues at the bottom left. Coinertia Analysis coefficients for environmental
340 variables (Y loadings) and morphological parameters (X loadings) at the two
341 graphs at the bottom right.

342

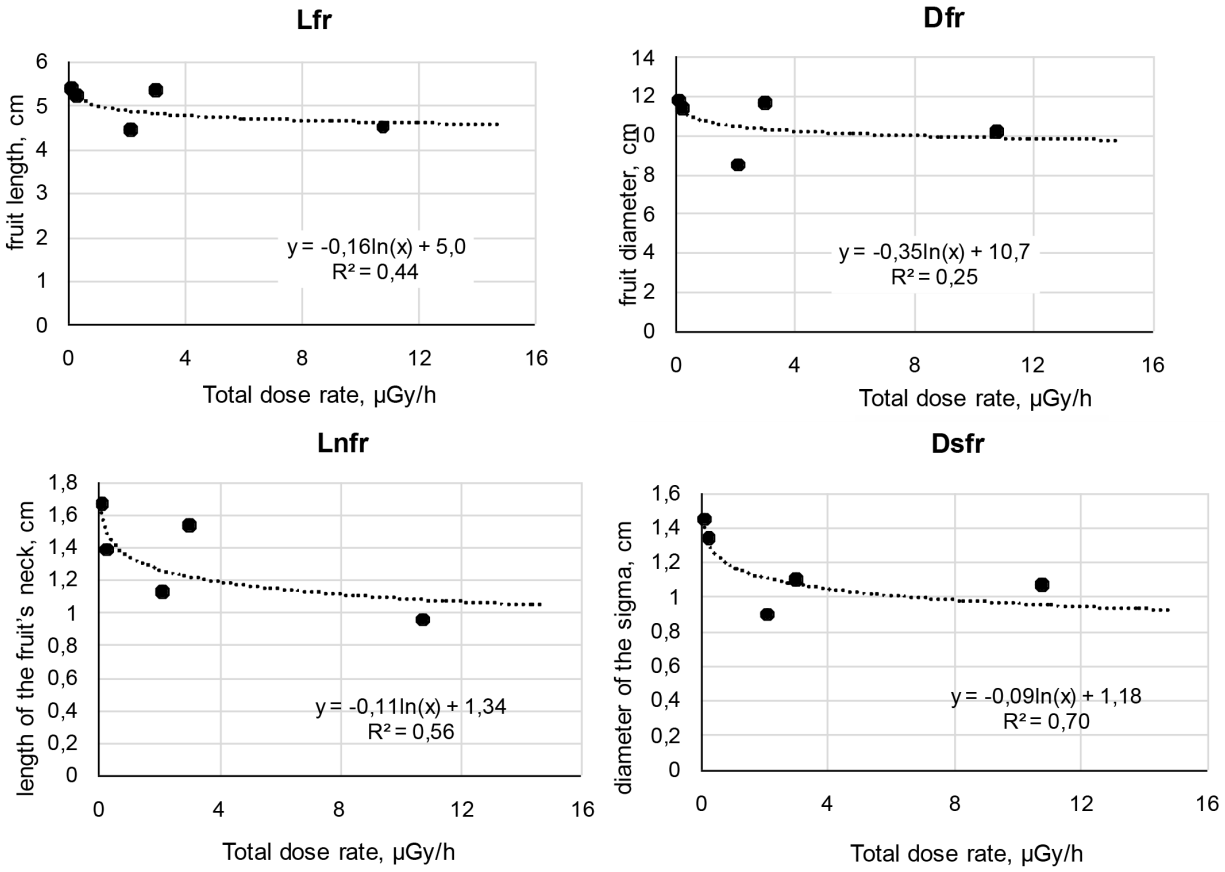

343 **Fig. 8.** Average morphological parameters of *Nuphar lutea* fruits in gradient of
344 radiation dose rate: Lfr – fruit's length, Dfr – fruit's width, Lnfr – length of the
345 fruit's neck, Dsfr – width of the fruit's neck.

346 As illustrated in the eigenvalues barplot, the first two Coinertia axes suffice
347 to describe the relationship between the structures of the studied morphological
348 parameters and environmental variables. Quantitatively, this relationship is
349 expressed by the RV coefficient, which was calculated to be 0.65.

350 Several groups of morphological parameters are identified at the bottom right
351 plot, X loadings, in Fig 7. The first two groups stretch along the first axis and consist
352 of Ls/Ws ratio, Wp, and Nsfr on the right side and Ws and Ls on the left side. High
353 values of Nsfr also rose with PO_4^{3-} content growth in the waterbodies. High values
354 of morphological parameters at the right side of the first axis are related to high NO_2^-

355 content and water mineralization level (see Y loadings in Fig.7) and probably with
356 low NO_3^- content, while the second group has an inverse relationship. The third
357 group consists of Dfr, Dsfr, and Nsr, which tend to be higher in water bodies with
358 low content of NO_3^-. The fourth group of parameters are Lnfr and Lfr that opposite
359 the sixth group, i.e., Lp and Lp/Wp ratio, which are associated with high and low
360 levels of radiation dose parameters respectively.

361 The studied water bodies are represented in the right top plot (Row scores
362 (X −> Y) in Fig. 7). The short arrows show a concordance between structures of
363 environmental composition and morphological parameters in each waterbody. The
364 Hlyboke Lake takes a separate position enabled by high radiation dose and PO_4^{3-}
365 content and is characterised by long Lp, large Lp/Wp ratio (the longest and one of
366 the widest pollen grains) and short Lnfr and Lfr (the smallest fruits with the shortest
367 fruit necks). These parameters have the highest loadings in the second component
368 and could be the indicator of radiation impact. In general, fruits dimensions did not
369 show a significant correlation with the total radiation exposure (Fig. 8).

370 Among the morphological parameters of fruits, only Lnfr and Dsfr
371 exhibited a dependence on the radiation dose rate, although other physicochemical
372 properties of water may have an effect. The morphological characteristics of a plant
373 greatly vary across their distribution range and depending on their habitat conditions
374 (Latowski et al., 2014). Therefore, direct comparisons with data from other studies
375 were not provided. Nevertheless, *N. lutea* fruit morphology in the CEZ's reservoirs
376 varies in a much wider range than those observed in previous research (Gudkov et

al., 2003). Aquatic macrophytes in the most heavily contaminated water bodies within the CEZ have displayed remarkable resilience despite nearly four decades of continuous exposure to ionizing radiation. There have been no substantial alterations observed in their plant community composition (Zub et al., 2023). Changes in composition of macrophyte communities inhabiting the shallow waters of CEZ reservoirs is predominantly influenced by hydrological factors, including degree of reservoir isolation, water depth, the presence of watercourses, and the rates of water exchange (Gudkov et al., 2003). Various morphological and physiological effects in macrophytes have been attributed to long-term exposure to low doses of ionising radiation (Gudkov et al., 2006; Gudkov et al., 2016; Iavniuk et al., 2020; Nurgudin et al., 2009; Yavnyuk et al., 2009).

Furthermore, radiation levels of up to 80 Gy that were reached in heavily contaminated water bodies immediately after the accident (Belyaev et al., 2020, 2023), may have induced genetic and chromosomal disorders in exposed plant cells. These instabilities could persist through many replication cycles, increasing the frequency of genetic alterations in subsequent generations. Cytogenetic investigations revealed an increased incidence of chromosomal mutagenesis in the cells of aquatic plants and animals in the CEZ (Car et al., 2023, 2022; Gudkov et al., 2016; Gudkov et al., 2009; Kesäniemi et al., 2018; Shevtsova and Gudkov, 2013; Tsyusko et al., 2006). Additionally, epigenetic regulations of genes expressions changes may also play a significant role in the response of plants to radiation exposure (Shevtsova and Gudkov, 2009).

399 Compared to other aquatic plants, *N. lutea* is characterised by low phenotypic
400 variability (Henriot et al., 2019; Schoelynck at al., 2014). However, determining the
401 plant's growth and size is challenging due to the effect of water depth and abundance
402 of clones, attributed to their substantial rhizomes. Hence, researchers usually focus
403 on traits independent of water depth and long-term individual development. These
404 traits typically pertain to recent plant growth, providing insights into the conditions
405 preceding sampling, particularly reproductive indicators.
406 The reproductive system of *N. lutea* shows a height sensitivity to
407 environmental stressors, rendering it more susceptible to external influences than the
408 plant as a whole (Mičieta and Murín, 1996). Thus, key indicators of a species'
409 sustainability encompass pollen viability and seed quality (Hjelmroos, 2000). Our
410 study further supports the significance of pollen fertility as an indicator of heavily
411 radionuclide-contaminated water bodies. Additionally, our results suggest that the
412 allometric Lp/Wp ratio is sencitive to relatively low-dose radiaton, bringing new
413 perspectives in the assessment of radoactively contaminated waterbodies.
414 The low fertility of pollen is evident solely in Vershyna Lake characterised by
415 absorbed dose rate, exceeding 14 μGy/h, which is most likely due to increased ^{90}Sr
416 incorporation in plants' tissues. The proportion of sterile grains in the samples here
417 was approximately 4.5 times higher than in the reference water body, while at other
418 sites we did not observe a significant lowering of pollen viability (see Fig. 4). This
419 implies that the reproductive system of *N. lutea* is relatively resistant to long-term
420 radiation exposure.

Vershyna Lake is situated at the center of the dammed area of the left-bank floodplain of the Pripyat River. This region has the highest activity concentration of ^{90}Sr in the CEZ, which is caused by the rewetting and waterlogging of the floodplain. Biologically available forms of ^{90}Sr are transferred from the soil of adjacent territories to the water bodies, followed by their accumulation in aquatic organisms (Gudkov et al., 2003; Gudkov et al., 2009).

The studied water bodies disappplayed more pronounced variations in the chemical composition of water and sediments than in the samples of *N. lutea* leaves, rhizomes, and roots (Tomaszewicz and Ciecierska, 2011). This inference is further supported by *N. lutea's* capability to accumulate higher concentrations of elements such as Ca, an analog of ^{90}Sr in a physiological context, in its organs than in surrounding water (Mazej and Germ, 2009; Polechońska et al., 2022; Tomaszewicz and Ciecierska, 2011).

In contrast, the allometric coefficient Lp/Wp increased gradualy in response to rising absorbed dose rates. In heavily contaminated reservoirs (Vershyna, Hlyboke, and Daleke lakes), this indicator exceeded the control sample by 10-13% (see Fig. 6).

As radioactive contamination increased, the size of *N. lutea* fruits and their morphological structures decreased. However, these parameters, showing a correlation with radiation dose rates, may be influenced by other physicochemical parameters of the water, particularly the content of biogens. For instance, Klok and van der Velde (2017) reported a significant positive relationship between water

phosphorus content and the number of flowers and seeds in *N. lutea*. These findings indicate that the reproductive success and productivity of the species tend to decline under nutrient-deficient conditions. In our study, we observed a substantial impact of the biogenic stressors on the reproductive structures of *N. lutea*, with approximately 65% of the variation in morphological parameters being attributable to environmental factors.

In cases where water bodies had higher PO_4^{3-} content, there was an associated increase in the number of seeds per capsule. Conversely, in water bodies with lower NO_3- content, larger seed capsules were formed, characterised by larger fruit diameters, stigma sizes, and the number of stigma rays.

4. Conclusions

This study revealed that reduced pollen viability and an increased pollen grain length-to-width ratio serve as indicators of high radiation exposure in *N. lutea*. Although pollen grains demonstrate relative resistance to long-term radiation exposure, in a water body with a radiation dose rate 176 times higher than the reference water body, we observed a 18% pollen sterility rate, which is 4.5-fold higher than in reference samples. A similar trend in pollen grain sizes was observed: the smallest pollen grains (with both length and width averaging lower values) were found in the reservoir with the highest external radiation dose rate, whereas in the remaining reservoirs, pollen grains were approximately 10-14% larger and exhibited

relatively consistent sizes. Conversely, the length-to-width ratio exhibited a distinct, gradual shift in response to increasing absorbed dose rates. In water bodies with substantial radioactive contamination, this indicator exceeded the control sample by 10-13%. The increase in radioactive contamination coincided with a reduction in fruit size and its associated morphological features in *N. lutea*. However, changes in fruit morphometric parameters were less dependent on the level of radiation exposure and probably influenced by a combination of factors which should be investigated further.

Funding

This study was supported by the National Research Foundation of Ukraine (Project No 2020.02/0264), the National Academy of Sciences of Ukraine, in cooperation with the State Specialised Enterprise "Ecocentre" of the State Agency of Ukraine on Exclusion Zone Management, and the MSCA4Ukraine (project number 1232738) funded by the European Union.

References

Arrigo, N., Bétrisey, S., Graf, L., Bilat, J., Gerber, E., Kozlowski, G., 2016. Hybridization as a threat in climate relict Nuphar pumila (Nymphaeaceae). Biodivers Conserv 25, 1863–1877. https://doi.org/10.1007/s10531-016-1165-z

Belyaev, V.V., Volkova, O.M., Gudkov, D.I., Prishlyak, S.P., Skyba, V.V., 2023. Radiation dose reconstruction for higher aquatic plants and fish in Glyboke Lake

during the early phase of the Chernobyl accident. J Environ Radioact 263, 107169. https://doi.org/10.1016/j.jenvrad.2023.107169

Belyaev, V.V., Volkova, O.M., Gudkov, D.I., Pryshlyak, S.P., 2020. Reconstruction of the absorbed dose of ionizing radiation for helophytes in the water bodies of the near emergency zone at the Chornobyl NPP. Nuclear Physics and Atomic Energy 21, 338–346. https://doi.org/10.15407/jnpae2020.04.338

Blasco, M., Badenes, M.L., del Mar Naval, M., 2016. Induced parthenogenesis by gamma-irradiated pollen in loquat for haploid production. Breed Sci 66, 606–612. https://doi.org/10.1270/jsbbs.16021

Butowt, R., Rodriguez-Garcia, M.I., Alchi, J.D., Gorska-Brylass, A., 1997. Calcium in electron-dense globoids during pollen grain maturation in Chlorophytum elatum R.Br. Planta 203, 413–421. https://doi.org/10.1007/s004250050208

Car, C., Gilles, A., Armant, O., Burraco, P., Beaugelin-Seiller, K., Gashchak, S., Camilleri, V., Cavalié, I., Laloi, P., Adam-Guillermin, C., Orizaola, G., Bonzom, J., 2022. Unusual evolution of tree frog populations in the Chernobyl exclusion zone. Evol Appl 15, 203–219. https://doi.org/10.1111/eva.13282

Car, C., Gilles, A., Goujon, E., Muller, M.-L.D., Camoin, L., Frelon, S., Burraco, P., Granjeaud, S., Baudelet, E., Audebert, S., Orizaola, G., Armengaud, J., Tenenhaus, A., Garali, I., Bonzom, J.-M., Armant, O., 2023. Population transcriptogenomics highlights impaired metabolism and small population sizes in tree frogs living in the Chernobyl Exclusion Zone. BMC Biol 21, 164. https://doi.org/10.1186/s12915-023-01659-2

De Storme, N., Geelen, D. The impact of environmental stress on male reproductive development in plants: biological processes and molecular mechanisms. Plant Cell Environ. 2014 Jan;37(1):1-18. doi: 10.1111/pce.12142.

Doledec, S., Chessel, D., 1994. Co-inertia analysis: an alternative method for studying species-environment relationships. Freshw Biol 31, 277–294. https://doi.org/10.1111/j.1365-2427.1994.tb01741.x

Dorken, M.E., Barrett, S.C.H., 2004. Phenotypic plasticity of vegetative and reproductive traits in monoecious and dioecious populations of *Sagittaria latifolia* (Alismataceae): a clonal aquatic plant. Journal of Ecology 92, 32–44. https://doi.org/10.1111/j.1365-2745.2004.00857.x

ERICA Assessment Tool 2.0,2023. The integrated approach seeks to combine exposure/dose/effect assessment with risk characterization and managerial considerations (http://www.erica-tool.com)

Fukuda, S., Iwamoto, K., Atsumi, M., Yokoyama, A., Nakayama, T., Ishida, K., Inouye, I., Shiraiwa, Y., 2014. Global searches for microalgae and aquatic plants

526 that can eliminate radioactive cesium, iodine and strontium from the radio-
527 polluted aquatic environment: a bioremediation strategy. J Plant Res 127, 79–
528 89. https://doi.org/10.1007/s10265-013-0596-9

529 Ganzha, Ch., Gudkov, D., Ganzha, D., Klenus, V., Nazarov, A., 2014.
530 Physicochemical forms of 90Sr and 137Cs in components of Glyboke Lake
531 ecosystem in the Chornobyl exclusion zone. J Environ Radioact 127, 176–181.
532 https://doi.org/10.1016/j.jenvrad.2013.03.013

533 Ganzha, Ch.D., Gudkov, D.I., Ganzha, D.D., Nazarov, A.B., 2020. Accumulation
534 and distribution of radionuclides in higher aquatic plants during the vegetation
535 period. J Environ Radioact 222, 106361.
536 https://doi.org/10.1016/j.jenvrad.2020.106361

537 Gudkov, D.I., Derevets, V.V., Kuzmenk, o M.I., Nazarov, A.B., 2003a. Radioactive
538 contamination of aquatic ecosystem within the Chernobyl NPP exclusion zone:
539 15 years after accident., in: Protection of the Environment from Ionising
540 Radiation. IAEA-CSP-17. IAEA, Vienna, pp. 224–231.

541 Gudkov, D. I., Kuzmenko, M.I., Derevets, V. V., Nazarov, A.B., 2003. Radioactive
542 contamination of aquatic ecosystem within the Chernobyl NPP exclusion zone:
543 15 years after accident, in: Protection of the Environment from Ionising
544 Radiation. IAEA-CSP-17. IAEA, Vienna. Vienna, pp. 224–231.

545 Gudkov, D.I., Kuzmenko, M.I., Kireev, S.I., Nazarov, S.I., Klenus, A.B., Kaglyan,
546 V.G., Kulachinsky, A.V., Zub, L.N., 2006. Radionuclides in components of
547 aquatic ecosystems of the chernobyl accident restriction zone, in: E.B.
548 Burlakova, V.I. Naidich (Eds.), 20 Years after the Chernobyl Accident: Past,
549 Present and Future. Nova Science Publishers, Inc., New York, pp. 265–285.

550 Gudkov, D.I., Nazarov, A.B., Kaglyan, A.E., 2009. Change of radionuclide
551 bioavailability in conditions of swamping territories within the Chernobyl
552 accident Exclusion Zone. Radioprotection 44, 951–955.
553 https://doi.org/10.1051/radiopro/20095170

554 Gudkov, D.I., Shevtsova, N.L., Pomortseva, N.A., Dzyubenko, E.V., Kaglyan, A.E.,
555 Nazarov, A.B., 2016. Radiation-induced cytogenetic and hematologic effects on
556 aquatic biota within the Chernobyl exclusion zone. J Environ Radioact 151,
557 438–448. https://doi.org/10.1016/j.jenvrad.2015.09.004

558 Gudkov, D. I., Uzhevskaya, S.F., Nazarov, A.B., Kolodochka, L.A., Dyachenko,
559 T.N., Shevtsova, N.L., 2006. Lesion in Common Reed by Gall-Producing
560 Arthropods in Water Bodies of the Chernobyl NPP Exclusion Zone.
561 Hydrobiological Journal 42, 82–88. https://doi.org/10.1615/HydrobJ.v42.i1.80

562 Gudkov, D.I., Zub, L.N., Savitskiy, A.L., 2002. Macrophytes of the Exclusion Zone
563 of the Chernobyl Nuclear Power Station: the Formation of Plant Communities
564 and Peculiarities of Radioactive Contamination of the Left-Bank Floodplain of
565 the Pripyat River. Hydrobiological Journal 38, 17.
566 https://doi.org/10.1615/HydrobJ.v38.i5.110

567 Henriot, C.P., Cuenot, Q., Levrey, L.-H., Loup, C., Chiarello, L., Masclaux, H.,
568 Bornette, G., 2019. Relationships between key functional traits of the waterlily
569 *Nuphar lutea* and wetland nutrient content. PeerJ 7, e7861.
570 https://doi.org/10.7717/peerj.7861

571 Hjelmroos, M., 2000. Interactions between Betula spp. Pollen and air pollutants, in:
572 Mat. of II Symp. Vienna, pp. 0–703.

573 Iavniuk, A.A., Shevtsova, N.L., Gudkov, D.I., 2020. Disorders of the initial
574 ontogenesis of seed progeny of the common reed (Phragmites australis) from
575 water bodies within the Chernobyl Exclusion Zone. J Environ Radioact 218,
576 106256. https://doi.org/10.1016/j.jenvrad.2020.106256

577 Jefferies, C.J., 1977. Sequential Staining to Assess Viability and Starch Content in
578 Individual Pollen Grains. Stain Technol 52, 277–283.
579 https://doi.org/10.3109/10520297709116794

580 Kashparov, V.A., 1998. Bulletin of Ecological State of the Restriction Zone and the
581 Zone of Compulsory (Mandatory) Evacuation.

582 Keddy, P., Gaudet, C., Fraser, L.H., 2000. Effects of low and high nutrients on the
583 competitive hierarchy of 26 shoreline plants. Journal of Ecology 88, 413–423.
584 https://doi.org/10.1046/j.1365-2745.2000.00456.x

585 Kesäniemi, J., Boratyński, Z., Danforth, J., Itam, P., Jernfors, T., Lavrinienko, A.,
586 Mappes, T., Møller, A.P., Mousseau, T.A., Watts, P.C., 2018. Analysis of
587 heteroplasmy in bank voles inhabiting the Chernobyl exclusion zone: A
588 commentary on Baker et al. (2017) “Elevated mitochondrial genome variation
589 after 50 generations of radiation exposure in a wild rodent.” Evol Appl 11, 820–
590 826. https://doi.org/10.1111/eva.12578

591 Klochenko, P.D., Kharchenko, G. V., Klenus, V.G., Kaglyan, A.Ye., Shevchenko,
592 T.F., 2008. 137Cs and 90Sr Accumulation by Higher Aquatic Plants and
593 Phytoepiphyton in Water Bodies of Urban Territories. Hydrobiological Journal
594 44, 48–59. https://doi.org/10.1615/HydrobJ.v44.i1.50

595 Klok, P.F., van der Velde, G., 2017. Plant traits and environment: floating leaf blade
596 production and turnover of waterlilies. PeerJ 5, e3212.
597 https://doi.org/10.7717/peerj.3212

Kurtar, E.S., 2009. Influence of gamma irradiation on pollen viability, germination ability, and fruit and seed-set of pumpkin and winter squash. African Journal of Biotechnology 8, 6918–6926.

Latowski, K., Toma, C., Dąbrowska, M., Zviedre, E., 2014. Taxonomic features of fruits and seeds of Nymphaea and Nuphar taxa of the Southern Baltic region. Limnological Review 14, 83–91. https://doi.org/10.2478/limre-2014-0009

Mazej, Z., Germ, M., 2009. Trace element accumulation and distribution in four aquatic macrophytes. Chemosphere 74, 642–647. https://doi.org/10.1016/j.chemosphere.2008.10.019

Mičieta, K., Murín, G., 1996. Microspore analysis for genotoxicity of a polluted environment. Environ Exp Bot 36, 21–27. https://doi.org/10.1016/0098-8472(95)00050-X

Møller, A.P., Mousseau, T.A., 2017. Radiation levels affect pollen viability and germination among sites and species at Chernobyl. Int. J. Plant Sci. 178, 537–545.

Møller, A.P., Shyu, J.C., Mousseau, T.A., 2016. Ionizing Radiation from Chernobyl and the Fraction of Viable Pollen. Int J Plant Sci 177, 727–735. https://doi.org/10.1086/688873

Mousseau, T.A., Møller, A.P., 2020. Plants in the Light of Ionizing Radiation: What Have We Learned From Chernobyl, Fukushima, and Other "Hot" Places? Front Plant Sci 11. https://doi.org/10.3389/fpls.2020.00552

Mulcahy, D.L., 1981. Pollen Tetrads in the Detection of Environmental Mutagenesis. Environ Health Perspect 37, 91. https://doi.org/10.2307/3429255

Murin, G., Micieta, K., 1998. Pollen grains as an indicator of environmental stress. Plant Ontogenesis in Natural and Transformed Environments 271–273.

Nurgudin, M.A., Shevtsova, N.L., Gudkov, D.I., 2009b. Effects of chronic low-dose radiation on the common reed within the Chernobyl accident Exclusion Zone. Radioprotection 44, 941–944. https://doi.org/10.1051/radiopro/20095168

Padgett, D.J., Les, D.H., Crow, G.E., 1998. Evidence for the hybrid origin of *Nuphar* × *rubrodisca* (Nymphaeaceae). Am J Bot 85, 1468–1476. https://doi.org/10.2307/2446403

Polechońska, L., Klink, A., Golob, A., Germ, M., 2022. Evaluation of Nuphar lutea as bioindicator of metal pollution in freshwater ecosystems. Ecol Indic 136, 108633. https://doi.org/10.1016/j.ecolind.2022.108633

Puijalon, S., Bornette, G., 2004. Morphological variation of two taxonomically distant plant species along a natural flow velocity gradient. New Phytologist 163, 651–660. https://doi.org/10.1111/j.1469-8137.2004.01135.x

Santamaría, L., 2002. Why are most aquatic plants widely distributed? Dispersal, clonal growth and small-scale heterogeneity in a stressful environment. Acta Oecologica 23, 137–154. https://doi.org/10.1016/S1146-609X(02)01146-3

Schoelynck, J., Bal, K., Verschoren, V., Penning, W., Struyf, E., Bouma T., Meire, D., Meire, P., Temmerman, S. 2014. Different morphology of Nuphar lutea in two contrasting aquatic environments and its effect on ecosystem engineering. Earth Surface Processes and Landforms. 39. 10.1002/esp.3607.

Shevtsova, N.L., Gudkov, D.I., 2009. Cytogenetic effects of long-term radiation on higher aquatic plants within the Chernobyl accident Exclusion Zone. Radioprotection 44, 937–940. https://doi.org/10.1051/radiopro/20095167

Thomaz, S.M., Esteves, F.A., Murphy, K.J., Dos Santos, A.M., Caliman, A., Guariento, R.D., 2009. Aquatic macrophytes in the tropics: ecology of populationsand communities, impacts of invasions and human use. Tropical Biology and Conservation Management 4, 27–60.

Tian, H.Q., Kuang, A., Musgrave, M.E., Russell, S.D., 1998. Calcium distribution in fertile and sterile anthers of a photoperiod-sensitive genic male-sterile rice. Planta 204, 183–192. https://doi.org/10.1007/s004250050245

Titus, J.E., Gary Sullivan, P., 2001. Heterophylly in the yellow waterlily, *Nuphar variegata* (Nymphaeaceae): effects of [CO_2], natural sediment type, and water depth. Am J Bot 88, 1469–1478. https://doi.org/10.2307/3558455

Tomaszewicz, H., Ciecierska, H., 2011. Changes in macroelement content in Nuphar lutea (L.) Sibith. and Sm. during the growing season. Acta Societatis Botanicorum Poloniae 78, 151–165. https://doi.org/10.5586/asbp.2009.020

Tsyusko, O. V., Smith, M.H., Oleksyk, T.K., Goryanaya, J., Glenn, T.C., 2006. Genetics of cattails in radioactively contaminated areas around Chornobyl. Mol Ecol 15, 2611–2625. https://doi.org/10.1111/j.1365-294X.2006.02939.x

Wells, C.L., Pigliucci, M., 2000. Adaptive phenotypic plasticity: the case of heterophylly in aquatic plants. Perspect Plant Ecol Evol Syst 3, 1–18. https://doi.org/10.1078/1433-8319-00001

Yuan, G., Li Z., Deng, J., Pacheco, J.P. and Fu, H. 2024. The performance and adaptation of aquatic plants under global changes. Front. Plant Sci. 15:1380921. doi: 10.3389/fpls.2024.1380921

667 Yavnyuk, A.A., Efremova, N.N., Protsenko, O.N., Gudkov, D.I., Nazarov, A.B.,
668 2009. Fluctuating asymmetry of zebra mussel (*Dreissena polymorpha* Pall.) and
669 floating pondweed (*Potamogeton natans* L.) in water bodies within the
670 Chernobyl accident Exclusion Zone. Radioprotection 44, 475–479.
671 https://doi.org/10.1051/radiopro/20095088

672 Zub, L.M., Prokopuk, M.S., Gudkov, D.I., 2023. Long-Term Observations over the
673 Structure of Macrophyte Communities in Floodplain Water Bodies of the
674 Chornobyl Exclusion Zone. Hydrobiological Journal 59, 39–53.
675 https://doi.org/10.1615/HydrobJ.v59.i2.30